Creating NbTiN thin films and designing the system to measure their critical temperature

Bachelor Thesis

R.P. van der Molen
11 062 061

Abstract

Superconducting thin films of niobium titanium nitride ($NbTiN$) are used for the detection of single photons. The films are grown atom by atom on an oxidized silicon wafer via a process called sputtering; a negative electric field is applied to the solid niobium and titanium in the vacuum chamber of the sputtering machine. This creates an ion bombardment from the argon and nitrogen gasses that are allowed inside. The bombardment hurls niobium and titanium atoms and/or clusters of atoms trough the chamber, where they settle on the chamber wall and the wafer. The 6 to 8 nm thick films are then processed into meandering nanowires by electron beam lithography.

The creating of the films involves a number of parameters that all have an effect on the properties of the film, and thus on the characteristics of the detector. Films created with fewer impurities tend to have a higher T_c, measuring the T_c of the created films is a suitable way to determine the quality of a film and thus a detector. A system is designed and assembled to measure the T_c of sputtered films. It consists of a cryo-head that uses compressed liquid helium to cool the samples down to ~ 2.5 K. Samples are placed under vacuum on oxygen free high conductivity copper ($OFHC$), and are electrically isolated from the copper mounting by a teflon sheet. Their resistance is calculated via a 4-point measurement.

To monitor the temperature inside the system a carbon ceramic resistor is placed inside. The resistance of this carbon, like any semiconductor, is temperature dependent because electrons move to the valance band at lower temperatures, increasing the resistance. A 50 Ω heating element is also placed inside and both this element and the carbon resistor are connected to a temperature control module which can be programmed to go from temperature A to B in steps of a given size. A Labview program was written that could combine the R, t-diagram obtained from the 4-point measurements and the T, t-diagram from the temperature control module into a R, T-diagram for up to eight channels at the same time to measure their T_c.

Films sputtered with higher substrate temperatures allow atoms to wiggle into place and form neat rows of atoms, increasing the T_c of the films. The thickness is another influence

of T_c; up to a certain thickness the thicker films show a higher T_c. Films should be sputtered around 80 nm thickness or higher and all have the same thickness to be compared correctly.

Contents

Chapter 1

Introduction

When cooled down to cryogenic temperatures an interesting phenomenon is observed in certain materials; their resistivity suddenly drops to zero and they become what is called 'superconducting'. One of these superconducting materials is Niobium Titanium Nitride ($NbTiN$). At the Royal Institute of Technology (KTH) in Stockholm, thin films of NbTiN, about a few nanometer thick, are produced with a technique called 'sputtering'. An AJA International ATC Orion Series Sputtering System [17] is used for this process. This machine has been operational for only a few months and the process to produce high quality NbTiN films is still in its early stage. During deposition parameters such as gas flow and ratio, as well as substrate temperature and plasma power can be changed. The effects of these parameters on the properties of the created thin films will have to be characterized and optimized.

This document contains a report on the influence of different parameters on the properties of the films, and the means to measure these properties. Special attention will be given to the measurement of the critical temperature (T_c) of the films. A system was specially designed and assembled for this measurement.

Chapter 2

Motivation

The Quantum Nano Photonics (QNP) research group's work at KTH focuses on the creation, manipulation and detection of single photons. Detection of single photons is done using a Superconducting Nanowire Single Photon Detector (SNSPD). It consist of a superconducting thin film, constructed into a meandering nanowire as is displayed in fig. 2.1. When energy is applied to a superconductor above a critical amount (I_c, T_c), the superconductive state is lost. A current is led trough the nanowire at $I = 0,95 \cdot I_c$. Incoming photons are absorbed by the meander (fig. 2.2a) and create a local resistive 'hot spot' (fig. 2.2b). Acting like a big rock in a river, the current has to flow around this hot spot, increasing the current density around it to $I > I_c$ (fig. 2.2c). Eventually the whole width of the wire is in a resistive state (fig. 2.2d), leading to a detectable pulse in the voltage. This pulse is registered and triggers a redirection of the current in external electronics, allowing the superconductive state to be restored and detect another photon in 20 ns.

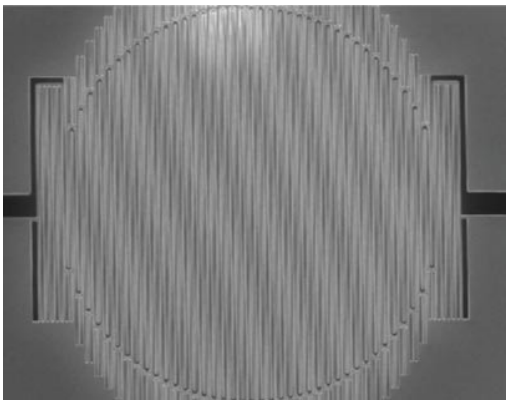

Figure 2.1: Meandering nanowire on an SNSPD.

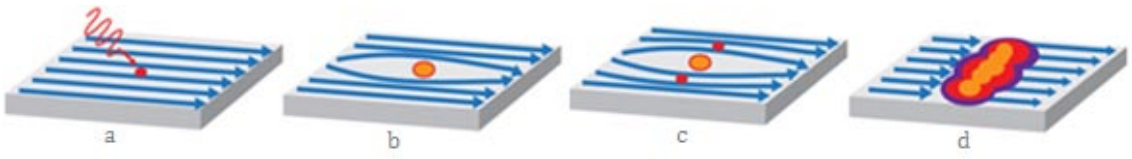

Figure 2.2: Operating principal of an SNSPD, the current running over the superconducting meander is represented by the blue lines.

The meandering superconductive nanowire on the SNSPD is etched out of thin niobium titanium nitride films. The creating of the films involves a number of parameters that all have an effect on the properties of the film, and thus on the characteristics of the detector. Films created with fewer impurities tend to have a higher T_c, measuring the T_c of the created way is a suitable way to determine the quality of a film. The idea is that detectors made from films with higher T_c will have higher detector efficiency.

Chapter 3

Sputtering NbTiN thin films

At KTH thin films of NbTiN are created using a sputter machine from AJA international (fig. 3.1[17]). It is located inside the cleanroom in the AlbaNova building at KTH to prevent contamination on the created film by dust particles. The properties of a sputtered thin film will depend greatly on the used settings during deposition (e.g. pressure, substrate temperature and plasma power). This chapter discusses the theory and procedure to create thin films of NbTiN and the machine they are created with.

3.1 The sputter machine

The machine consists of two vacuum chambers separated by a manual valve; the main chamber where the sputtering is done and the load-lock that prevents that vacuum in the main chamber has to be broken every time a sample is loaded. The sputter process (described in section 3.2) requires a high vacuum to prevent contaminants from inhibiting the created film. A turbo molecular vacuum pump [3] is attached to the load-lock that uses spinning fans at 1500 Hz to physically hit atoms out of the chamber. The turbo pump needs a mean free path of air to be ~ 0.7 mm to work effectively, herefor a roughing pump [4] is used to initially bring the pressure down to $\sim 10^{-3}$ Torr (1 Torr = 1.33 mbar). The main chamber uses a Cryo-Torr Cryopump [14] that uses 2 stages with different temperatures to allow gasses to condensate and/or be adsorbed on the surface. At very low pressure atoms have more interaction with the walls than with each other due to their mutual distance, a cryo-pump is more effective in creating a vacuum under these conditions. The first array is around 80K and

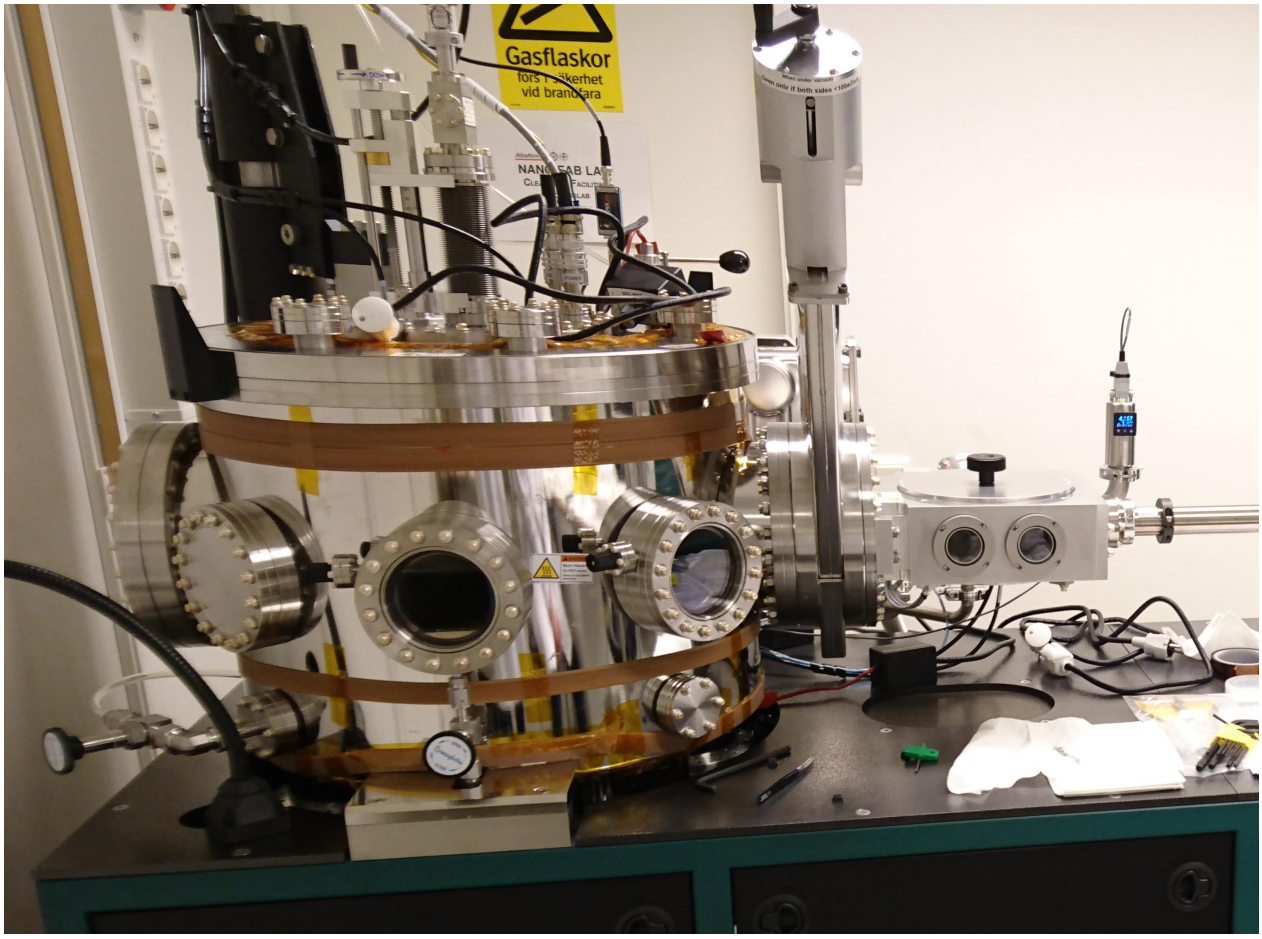

Figure 3.1: AJA sputtering machine, with on the left the main vacuum chamber and on the right the load-lock.

the second array is around 15K. The 80K condensing array condenses water and hydrocarbon vapors. The 15K array condenses nitrogen, oxygen, and argon while the specially processed charcoal of this array traps helium, hydrogen, and neon, pumping it to 10^{-9} Torr.

Gas flow in the system is measured in standard cubic centimeters per second (sccm). Two inlets can provide a regulated flow for the argon (1 <sccm 100)and nitrogen (0.2 < sccm < 20) in the main chamber with an accuracy of ± 0.1 sccm. Argon is an inert noble gas which only serves to provide ions for the ion bombardment, nitrogen is a reactive gas that will bind to the niobium and titanium. To initiate and sustain the plasma, and thus the sputtering, the A3DC power supply provides three 600W direct current (DC) power generators that can operate simultaneously. Two radio frequency (RF) power supply's are also included,

typically around $13 - 14$MHz. One RF power supply is 300W for when the sputtering of insulating materials is desired [15]. Insulating materials tend to accumulate charge and the alternating current (AC) alleviate this problem because positive charges accumulated during one half-cycle can be neutralized by electron bombardment during the next cycle. There is also one 50W RF source available to create a local plasma at the substrate to clean it before deposition.

The required materials needed for sputtering are present in the form of solid 'targets' at the bottom of the main chamber (fig. 3.2 (right)). They are placed on a magnetic ring that guides the free electrons in the plasma in a set trajectory as is displayed in fig. 3.2 (left). This way the electrons are focused in a certain area and have a higher probability to hit another electron from the outer shell of an argon atom in the plasma. This way the plasma is sustained. A grounded shield surrounds the target, this shield is water-cooled to diminish the risk of flaking on the target. Flaking happens because the target material that is constantly sputtered on the grounded shield comes loose in flakes due to thermal expansion and retraction that takes place during a sputter session. Flakes that come loose can short-cut the target with the chimney and prevent the sustainability of the plasma.

Targets are covered by a shutter to contain the plasma if needed. There are separate

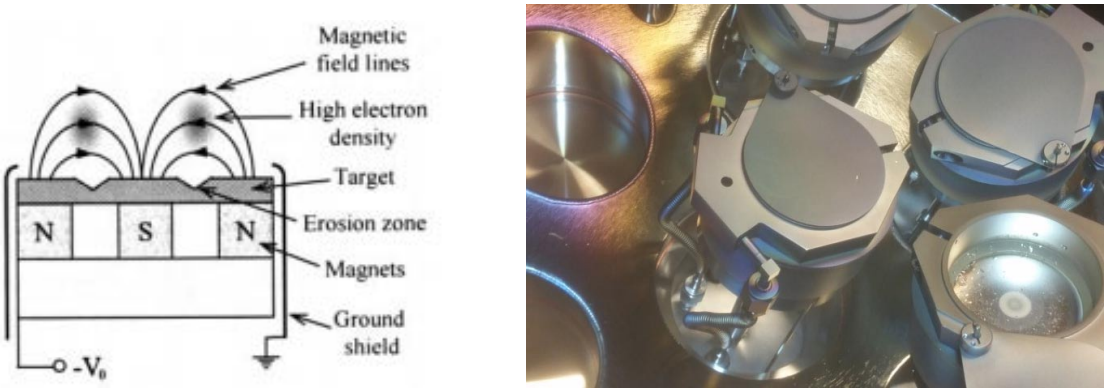

Figure 3.2: Left: schematic drawing of a magnetron configuration [2]. Right: top-view picture of the targets inside the main chamber, the shutter covering the titanium target (bottom right) is open.

targets for niobium (Nb) and titanium (Ti). The Nb target is situated directly perpendicular under the substrate holder, but for the Ti target there is no room directly under the substrate holder and so it is positioned under an angle so it is still pointing towards the substrate. By having two different targets both can be controlled independently and the stoichiometry of the created film is better under control.

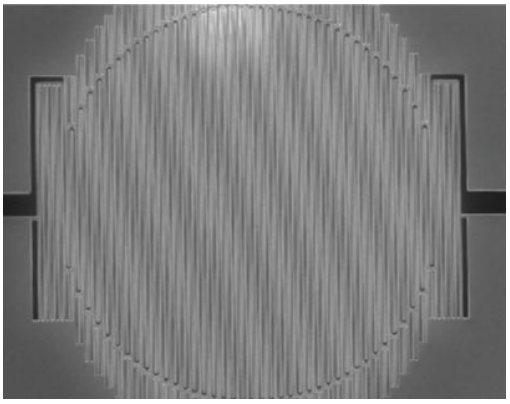

Figure 3.3: Meandering nanowire on an SNSPD.

At the center of the ceiling in the main chamber there is a mechanism to lock the substrate-holder into place. This mechanism can rotate at 1 Hz to provide better uniformity in the deposited film. A SHQ-4X [9] series substrate heater, capable of heating the substrate to $850 \pm 2°C$ is also attached to the substrate holder. The temperature is monitored and controlled with an Ogden ETR-9300 [10] temperature control module. To get the substrate holder from the load-lock to the main chamber an arm is used that can be moved using magnets so the vacuum does not have to be broken. Windows are situated on 2 places of the main chamber as can be seen in fig. 3.1. One to see inside, and one to get light inside. The view from the outside can be blocked by a shutter on the inside with magnets. This is done during sputtering so the shutters collect the sputtered material instead of the windows. The film growth can be monitored with a SQM-160 Thin Film Deposition Monitor which is located in the main chamber near the substrate. It uses a vibrating piezo-electric quarts crystal. When atoms condense on this crystal the added mass changes the frequency at which the crystal vibrates. The change in frequency (Δf) can be correlated to the added mass (Δm) via Sauerbrey's equation [7]:

$$\Delta f = -\frac{2f_0^2}{A\sqrt{\rho_q \mu_q}} \Delta m \tag{3.1}$$

where f_0 is the resonance frequency in Hz, A is the surface area of the piezo crystal in cm^2,

ρ_q is the density of the quartz crystal in $g \cdot cm^{-3}$ and μ_q is the Shear modulus ($2.947 \cdot 10^{11}\, g \cdot cm^{-1} \cdot s^{-2}$). With the added mass and the atomic density of the sputtered material the thickness of the created film can be calculated. Calculating the deposition rate is done by the instrument. It requires the density and the Z-factor of the material that is sputtered. The Z-factor is used to match the acoustic properties of the material to those of the crystal. When the deposition rate measured by the instrument is not consistent with the one checked after deposition with other means, a tuning factor can be inserted to correct this [6]:

$$F_m = F_i \frac{T_m}{T_i} \tag{3.2}$$

where F_m is the modified tuning factor, F_i is the initial tuning factor, T_m is the measured thickness by external instruments and T_i is the measured thickness by the internal instrument. The first films sputtered resulted in a thickness of 10.3 nm thickness, while the profilometer measured a height difference between the substrate and the sputtered layer of 9.2 nm. The old tuning factor of 148 was replaced by the new value of 132 to compensate.

3.2 Deposition of NbTiN

This section explains the procedure to create thin films of NbTiN, using the machine discussed in the previous section.

3.2.1 Preperation

The substrate for the NbTiN film is a (piece of) oxidized silicon (SiO_2) wafer. The oxidized layer reduces lattice mismatches between the substrate and the sputtered NbTiN [36] Before loading these on the sample holder they undergo a sonic bath submerged in acetone for three minutes at room temperature to remove any unwanted dust particles from their surface. When they come out of the bath the acetone is washed off with isopropanol (IPA). The substrate samples are then loaded on a sample holder and placed in the load-lock, the turbo pump is switched on and when a pressure of $< 5 \cdot 10^{-6}$ Torr is reached the door between both vacuum chambers can be opened. A small argon flow is let in to the main chamber to apply a higher pressure there, so when the door is opened the air current flows towards the load lock to prevent contamination in the main chamber. The substrate-holder is locked into place at the center of the ceiling of the main chamber. The cryo-pump then pumps the main chamber to $< 5 \cdot 10^{-8}$ Torr before pre-sputtering can begin.

3.2.2 Deposition

Sputtering is a process during which a positive ion bombardment causes the atoms on whats called a target, to come loose and stick on a substrate. When the pressure in the main chamber is $< 5 \cdot 10^{-8}$ Torr, enough contaminated air is deemed pumped out of the main chamber. Next a pressure of 30 mTorr is applied by allowing a mixture of argon (Ar) and nitrogen (N_2) gas in the chamber. The door between the main chamber and the cryo-pump will

automatically open and/or close depending on the gas flow, the current- and desired pressure. When gas flow and pressure are in equilibrium the gas can be ignited into a plasma by applying an electric field [1]. The electrons and the nucleus of the gas atoms will be pulled from each other, creating loose electrons and ions; a plasma (fig. 3.4). The plasma is now conductive and will emit a glow that is caused by (de)ionising atoms. The wavelength of this glow is dependent on the amount of energy an ionized atom looses when de-ionising. After ignition of the plasma the pressure will be changed to 3 mTorr. A higher pressure will allow an easier ignition of plasma but influences the mean free path of the target atoms during sputtering. Higher pressure will prevent some target atoms to reach the substrate due to collisions with particles in the plasma. The critical temperature, resistivity and stress on the created films seems to worsen as the pressure goes up from 3 mTorr [23]. A lower pressure results in a more directive deposition because the mean free path of the target atoms is longer. A pressure of 3 mTorr will therefore be maintained while sputtering.

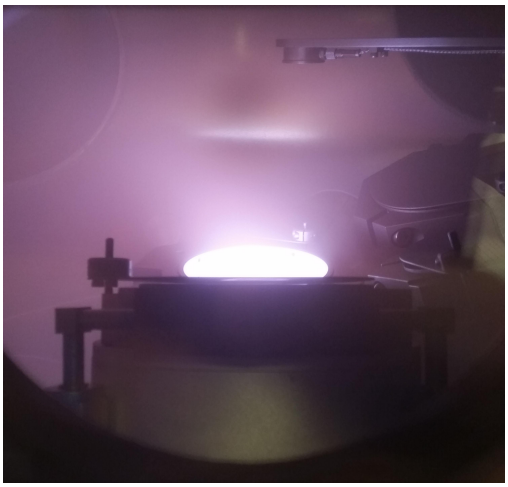

Figure 3.4: Picture taken from NbN plasma in the main chamber, with top-right the thickness monitor.

The negative charge applied to the targets to ignite the plasma repels the free electrons present there. They are repelled from the target to the substrate and trapped by the magnetic field surrounding the target. On their way they collide with the argon atoms and drive the outer shell electrons from the nucleus, creating argon ions: $Ar + e^- \rightarrow Ar^+ + 2\,e^-$. The extra electrons created in this process can collide with other argon atoms again, creating a cascade process of ionization [5]. While the electrons are repelled from the target by the applied electrical field, the positive argon ions will immediately be accelerated to the Nb or Ti target. They collide with the target material and in the process loose atoms, clusters of atoms or molecules of Nb and Ti will be flung away towards the substrate as is displayed

in fig. 3.5. The magnetic field ensures that the electrons are not capable of bombarding the substrate, and at the same time enhances the probability of ionizing a neutral gas molecule in the plasma by several orders of magnitude [18]. The result is a higher deposition rate on the substrate. During their travel the atoms can collide with various materials inside the plasma, resulting in deposition in all angles. The collision will also create more free electrons from the target, which will further sustain the plasma.

After the plasma is ignited, over the course of two minutes the power is then ramped up to the desired value ($\sim$ 300 W). During this time the shutter blocking the sputtered atoms from reaching the substrate is closed. Ramping the power with the shutter closed has the benefit of not putting a lot of sudden strain on the target and also cleans the target surface of any impurities. This process is called pre-sputtering. When the power is at the set value, first the thickness monitor is put into position, then the shutter is opened and sputtering on the substrate can commence. When the desired thickness of the film (or the time sputtered) is reached, the shutter is closed and the is power ramped down to 50 W and subsequently turned off. The sample holder can now be unloaded via the load-lock once it is at atmospheric pressure.

When the substrates are loaded they will be attached to the substrate holder which in turn is attached to a locking mechanism which can rotate to improve uniformity of the created film. The distance the substrate will have from the target can be altered. This is also done during the process to lock the sample holder in place. Because the titanium target

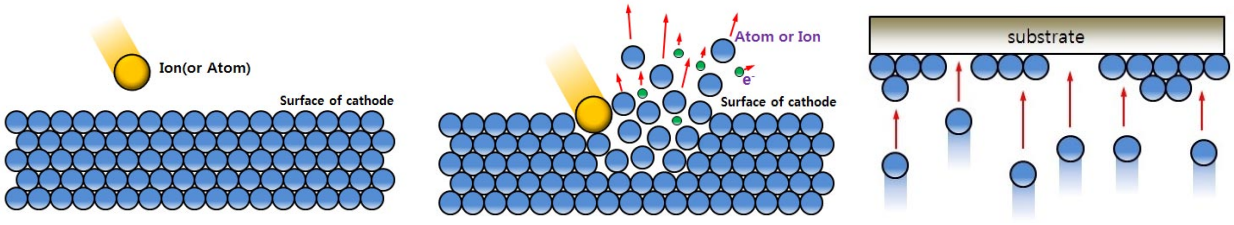

Figure 3.5: Left: argon ion flying to target material. Mid: argon ion colliding with target material. Right: atoms of target material condense on the substrate [20].

is placed in an angle towards the substrate, the substrate holder will be put at 10mm from the maximum height. This way the films will be produced more homogeneously.

From the chapter above can be concluded that creating thin films with a sputter machine is a dynamic process that involves a lot of parameters. This is however why this process is so potent; being able to control each parameter very precise allows for fine tuning the final product in the desired composition.

3.3 Encountered problems

Flaking was detected in the Nb target after the plasma did not ignite. Clearing this problem resulted in a leak in the main chamber, the pressure did not reach desired values of 10^{-8} mTorr. The leak was not originating from dust on the o-rings that seal the lid on the main chamber, this was thought to be the most common cause. A residual gas analyzer was purchased that ionizes atoms and molecules and sorts them by mass to charge ratio. It was found that there was an abnormal amount of water present. Checking the water cooling of the targets confirmed the leak (fig. 3.6). With a lot of water contaminants in the chamber the produced films will also contain these contaminants and the decision was made to not produce films until the problem is solved. The system can not operate with the water cooling not running, this is a fail safe intended to prevent overheating of the targets during sputtering.

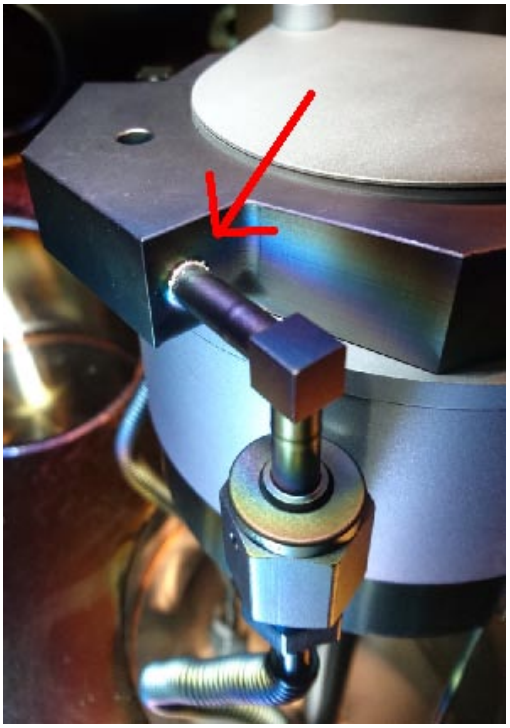

Figure 3.6: Damage to the water pipe leading to the target cooling.

Chapter 4

Measuring the critical temperature of a superconductive thin film

One property of a superconductor is its critical temperature (T_c), when cooled below this temperature a superconductor becomes superconductive. This chapter discusses the basic principle behind superconductivity and the process to design and assemble a system to test the T_c of the created thin NbTiN films.

4.1 Superconductivity

Discovered first in 1911 by H. Kammerlingh Onnes, superconductivity is a material property that shows appears at low temperatures. Superconductive materials exclude magnetic fields from their body (Meissner effect) and have zero resistivity. They are divided into two catagories; type I and type II superconductors. Type I superconductors are made from single elements and their superconductive state completely breaks down when an induced magnetic field (H) becomes larger then a critical value (H_c). Type II superconductors are made from alloys and exhibit the same properties of type I superconductors except that they allow for magnetic fields to locally penetrate when $H > H_c$.

When a superconductive material cools down, at a certain temperature the lattice vibrations inside the metal diminish enough for passing electrons to attract and move the positive nuclei closer together. This will result in a locally higher positive electrical field

which will attract another nearby electron (fig. 4.1). Both electrons form a Cooper pair [22] which encounters no resistance while passing trough the metal. When one of the electrons in a Cooper pair encounters an impurity and scatters off, it will quickly connect with other (Cooper paired) electrons.

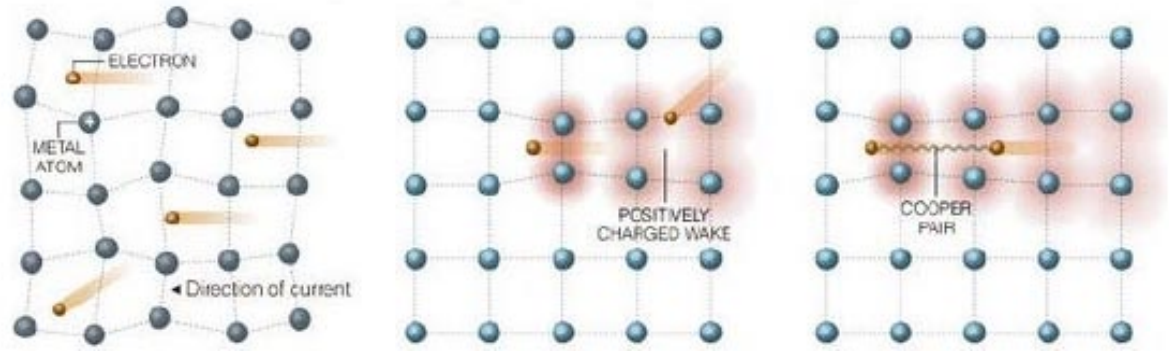

Figure 4.1: Left: electrons move trough a metal at $T > T_c$ and encounter resistance from vibrating lattices. Mid: at $T = T_c$ lattice vibrations slow down enough for passing electrons to attract positive nuclei, creating a locally relative larger positive field that attracts another nearby electron. Right: two electrons form a cooper pair [19].

4.2 Samples at cryogenic temperatures

To reach the superconductive state in the samples they have to be cooled down to $T < T_c$. The cooling down is done by a RDK-101 cryogenic cold-head from the compagny Sumitomo. It uses compressed helium to cool two stages to cryogenic temperatures. To minimize heat exchange between the samples and the environment by convection the samples are placed in a vacuum chamber and pumped to $\leq 5 \cdot 10^{-8}$ atm. A shield is attached to the first stage ($\sim 40K$) that covers the samples and blocks thermal radiation from reaching the samples fig. 4.2.

The samples have to be thermally connected to the cold-head to reach their superconductive state. A mounting is made from oxigen free high conductivity copper ($OFHC$). OFHC is copper with $>$ 99.90 % purity and a $<$ 0.001 % oxygen content , and a high thermal

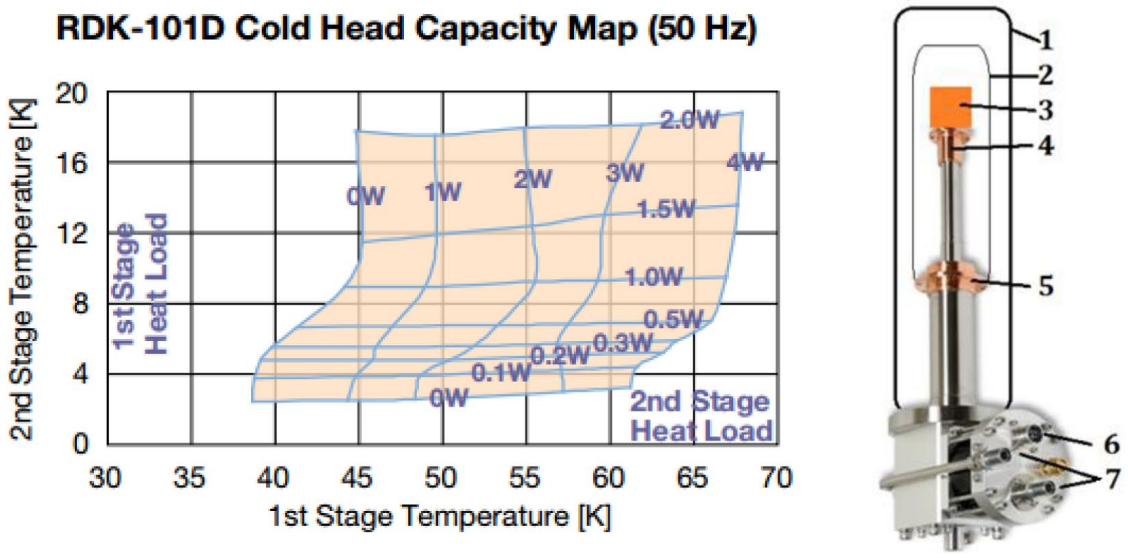

Figure 4.2: Left: capacity map for the RDK-101D cold head from Sumitomo, different amounts of energy leaking will result in different temperatures at both stages. Right: the cold-head pictured with: (1) Vacuum shield, (2) heat shield, (3) sample mount, (4) second stage, (5) first stage, (6) power plug, (7) helium entrance and exit [42].

conductivity [32]. To minimize wear and tear on the system due to loading and unloading samples, a bottom and a top part are designed to hold the samples. Both are displayed in fig. 4.3. The bottom part will be a 4 mm thick disc with a diameter of 85 mm. Thread-free holes will be implemented to attach it to the cold-head. The disc will contain eight slots to allow spring loaded pins [31] that make contact on the samples to the measuring electronics. The pins are kept in place with two component epoxy resin [12] that is suited for cryogenic environments. One component is the epoxy resin and the other is an catalyst to start homopolymerisation, gluing the resin to itself and to the copper mounting. The top part of the OFHC mount is the part where the samples are clamped. The silicon wafer on which the NbTiN is sputtered is superficially oxidized on both sides with silicon dioxide (SiO_2). Because this is an excellent electrical insulator only the sides will have to be insulated to perform the resistance measurement correctly. Samples are clamped with the same insulating material which only leaves place for the pins to make contact.

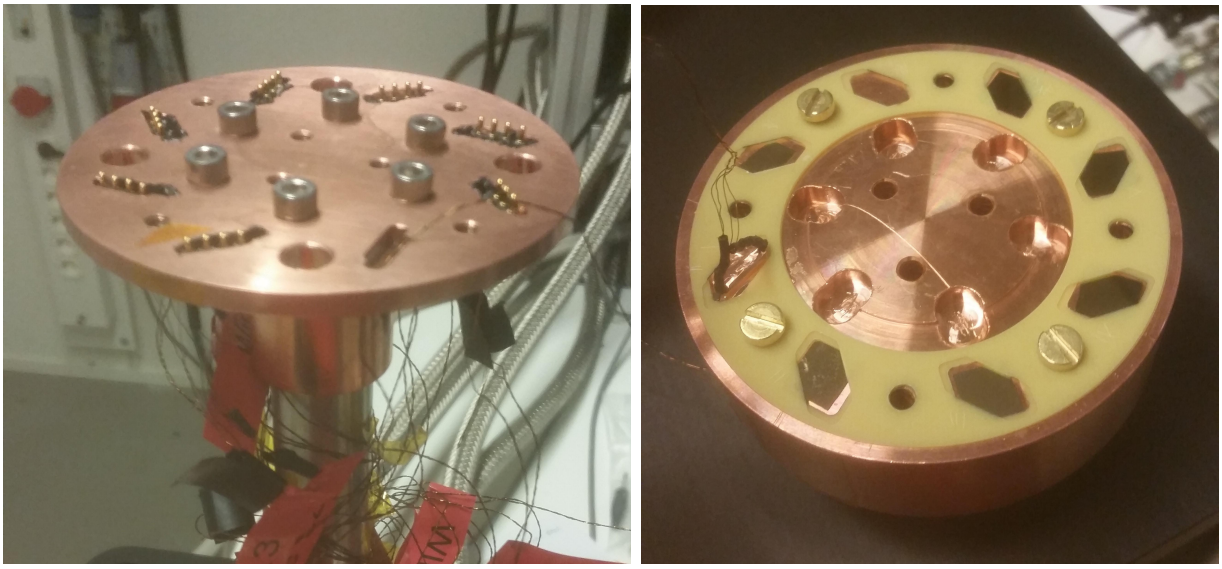

Figure 4.3: Left: Bottom part of the sample holder mounted to the 2nd stage of the cryo-head. Right: Top part of the sample holder, including clamped samples and on the left the ccr. Screws used to clam the bottom part on the cold head fit into cavities on the top part.

4.3 Data acquisition

4.3.1 Hardware

To control and measure the temperature inside the system a Cryocon heating element [**?**] and a carbon ceramic sensor (CCS) [40] are attached to the top part of the mount. Both are connected to a Lakeshore 331 Temperature controller [43]. This controller can be programmed to go from temperature A to B in steps of a given size. The heating element placed inside the system provides control over the temperature when the system needs to warm up. The Model 331 heater output current source has a maximum output of 1 A and a voltage limit of 50 V. Both limits are in place at the same time, so the smallest of the two computations gives the maximum power available to the heater. Trough Ohm's the maximum power, and most efficient heating element is achieved when the heating element has a ideal resistance of:

$$P_{max} = A^2 \cdot R = \frac{U^2}{R} \qquad \rightarrow \qquad R = \frac{U}{I} = 50\,\Omega. \tag{4.1}$$

The temperature is measured with the CCS. Carbon has, as every semiconductor, an energy gap between the valence and conductive bands. At higher temperatures more electrons inhibit the conductive band, decreasing the resistance. At low temperatures the electrons move to the valence band and cause the carbon to have a higher resistance, as can be seen in fig. 4.4. The ceramic used in the ccs thermometer provides high thermal conductivity and electric isolation for the carbon. 10 μA is channeled trough the resistor and the voltage is measured to calculate the resistance. Subsequently the temperature is calculated using the polynomial fit. The calibrated resistor comes with a measured R,T-curve with a polynomial fit that can be imported into the Lakeshore. The temperature will automatically be measured with an accuracy of $\pm$ 12 mK at cryogenic temperatures. The sensor is placed in a slot for a sample to get the most accurate temperature reading for the samples as possible.

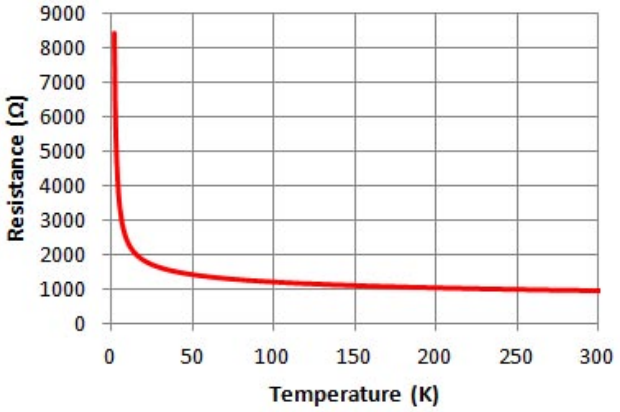

Figure 4.4: Plotted R,T-curve from the data points supplied with the carbon ceramic sensor from Temati [40].

Measuring the transition from the conductive to the superconductive state is done with a 4-point resistance measurement [29]. Rather then measured, the resistance is calculated with ohm's law ($R = U/I$) by applying a constant current through the sample and measuring the voltage across it. The name of this measurement relates to the 4 points that have to be connected to the sample (fig. 4.6). The big advantage of a 4-point over a normal resistance measurement is that the resistance of the wire's leading to and from the sample will not be taken into account. Especially at lower values this increases the inaccuracy. When the superconductive state is reached a drop in resis-

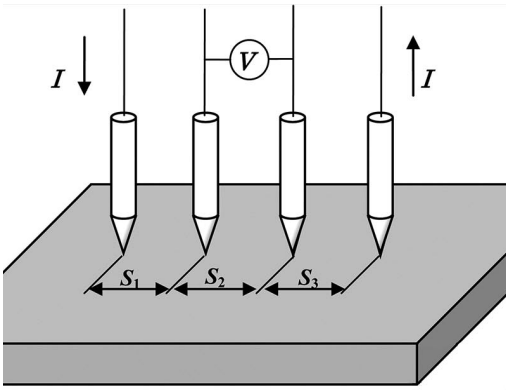

Figure 4.5: Scematic of a 4 point measurement ($S_1 = S_2 = S_3$) [29].

tance, and thus voltage, is expected. With this 4-point measurement the sheet resistance of the film can also be calculated at T_r and at $T < T_c$. The resistivity ρ is dependent on the measured voltage and current and factor C' that is applied for the geometry of the sample. C' depends on the width a and depth d of the sample, and the spacing s between the four probes. For our sample where $d/s = 5$ and $a/d = 1$, $C' = 3.5098$ [30].

$$\rho = \frac{V}{I} \cdot 3.5098 \tag{4.2}$$

The resistivity of the samples, when measured with the 4-point measurement, greatly depends on its geometry. Samples were cleaved with an apparatus that uses a diamond tip to scribe a line on the wafers. Afterwards the line will form a fracture when force is applied on both ends of the sample. Some samples had to be re-cleaved after the T_c measurement setup was finalized because they did not fit. Cleaving smaller samples may break them This resulted in different geometries and thus a resistivity that is difficult to relate. However the transition between normal and superconductive state can still be measured.Quad-twisted phosphor bronze wires with a 36 American Wire Gauge (AWG) diameter (d$=$ $0,127\,$mm) from Lakeshore (QT-36 [44]) conduct signals and current inside the vacuum system. The chosen material and small diameter mini-

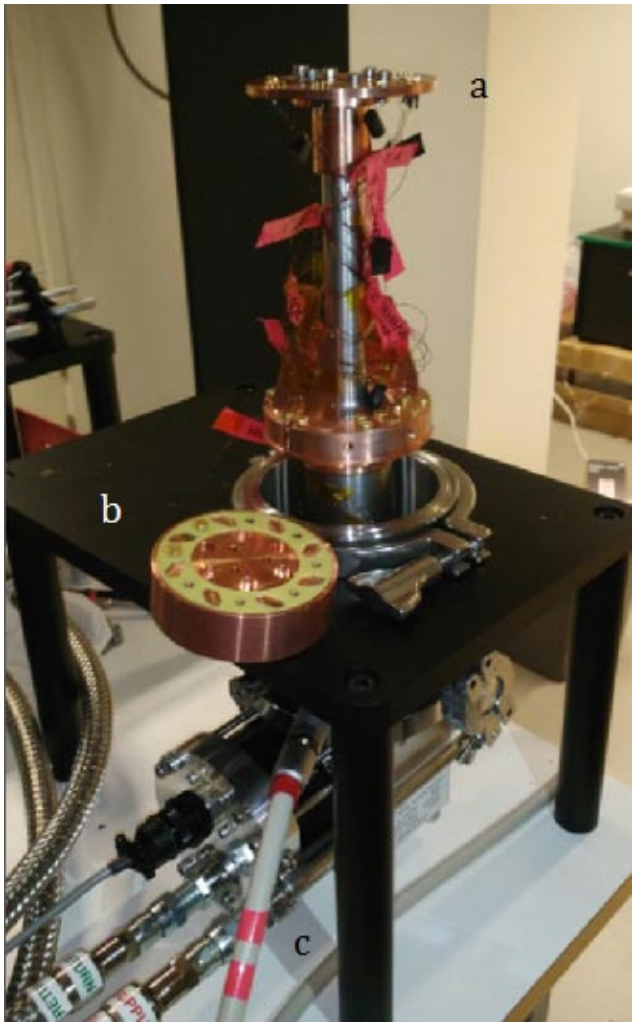

Figure 4.6: Measurement setup with a) the bottom part of the sample mount, b) the top part of the sample mount and c) helium inlet and outlet for the cryo-head.

mize heat-conductivity, and maximize electrical conductivity to the samples. The QT-36 wire consists of two pairs, each pair incorporates 3.15 twists per centimeter, and the 2 pairs are entwined at 1.57 twists per centimeter. Twisting the cables cancels out electromagnetic interference from external sources and improves the accuracy of the diode and 4-point measurements. The 4-point measurements will be done by a Keithley Series 2700 Multimeter/Data Acquisition/Switch System [33]. It has a build-in function for 4-point resistance measurements and allows for a Keithley 7700 Differential Multiplexer Module (fig. 4.7 [34]) to be connected at the rear for up to ten 4-point resistance measurements to be done simultaneously. The multiplexer uses mechanical switches with a lifetime of $> 10^8$ switches. With a sample frequency of 1Hz, eight channels can be measured continuously for twenty weeks. This relates to $>$ 3000 measurements.

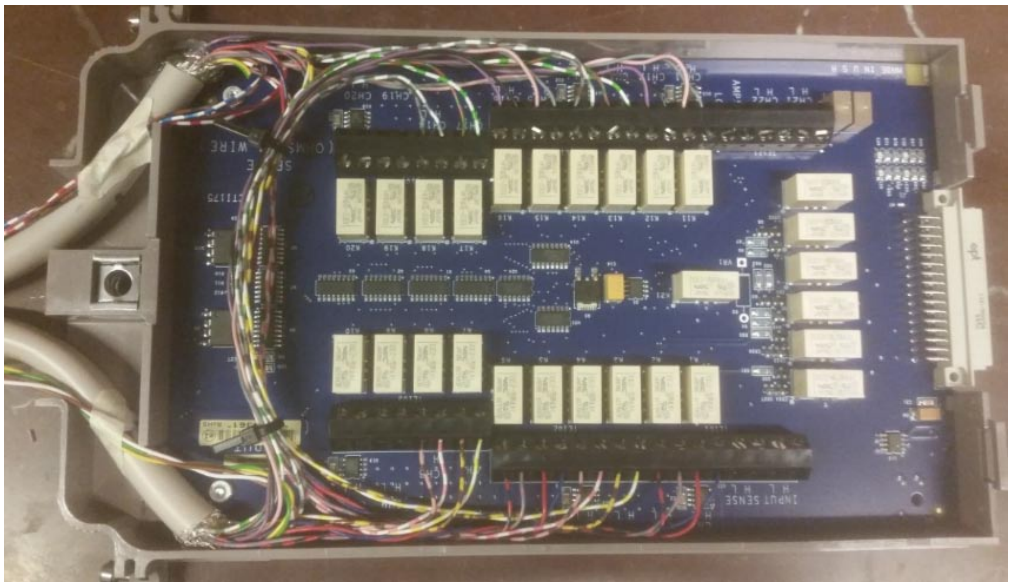

Figure 4.7: Keithley 7700 multiplexer module with connected wire's leading to the T_c measurement setup to perform the 4-point measurement. The top part of the card provides the current and the bottom part measures the voltage.

4.3.2 Software

Both the Lakeshore temperature control module and the Keithley data acquisition system are connected to a computer via USB. A Labview program was written in collaboration with T. Lettner (PhD student in the QNP group), that could combine the R, t-diagram obtained from the Keithley and the T, t-diagram from the Lakeshore into a R, T-diagram for up to eight channels at the same time to measure their T_c as is displayed in fig. 4.8. The temperature and resistance can be measured independently. This way the process of cooling down the samples can be monitored without having to use the switch system.

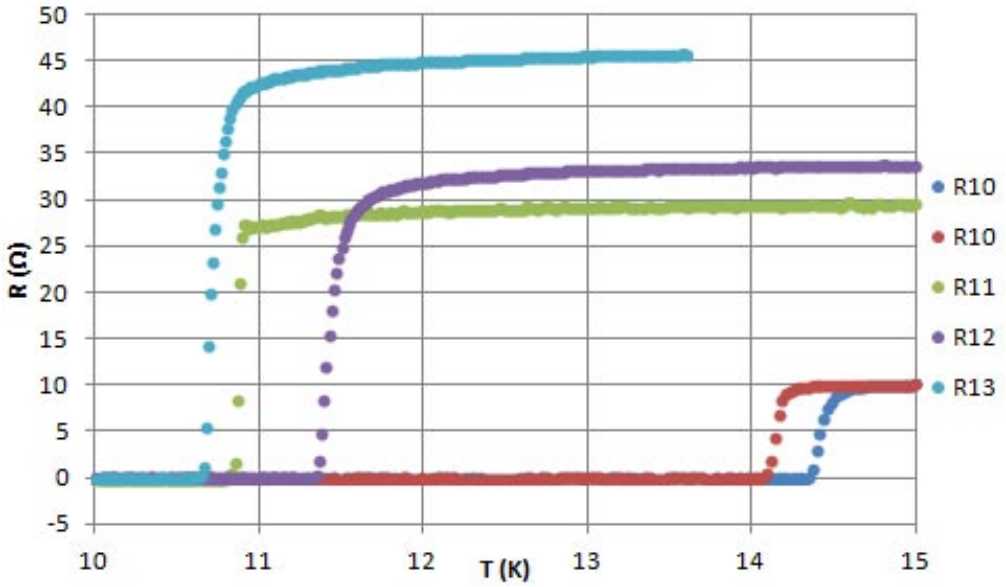

Figure 4.8: R,T-curve for samples R10-13 made from data obtained with the designed T_c measurement setup.

Chapter 5

Influence of sputter parameters on the critical temperature of a thin film

This chapter discusses the various experiments undertaken to characterize the influence changed parameters (fig. 5.4) during sputtering have on the properties of the created thin film. The theory is explained and results are presented in fig. 5.5.

5.1 Film properties

A film is grown atom by atom inside the sputter machine. The deposition rate is obtained by checking the thickness of the created film and dividing it by the time that it has been sputtered. This rate is important because future applications of the film will need a certain thickness to operate efficiently. Additionally, T_c of a thin film is dependent on its thickness up to a certain point (fig. 5.1). Lines are applied on the substrate with a permanent marker before sputtering, which are afterwards lifted off with acetone during a sonic bath. This removes sputtered material on the marker lines, revealing the surface of the substrate. Film thickness is measured with a profilometer [38]. A stylus is moved along the sample in one dimension and the

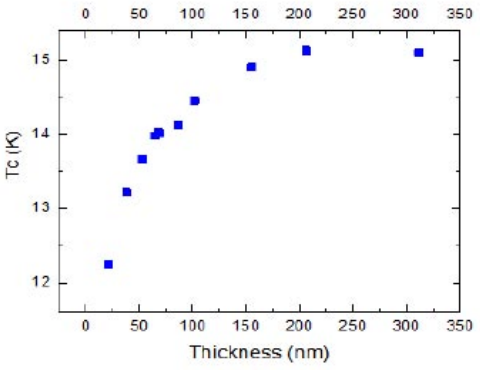

Figure 5.1: The thickness of a thin NbTiN film has influence on its T_c [16].

profilometer measures small surface variations in vertical stylus displacement as a function of position, placing the data in a graph real time. After measurements two point linear modifications can correct for any slanting.

Surface profile of the created film was measured with an Atomic Force Microscope (*AFM* [39]). The AFM was invented by G. Binnig in 1986 [41] and incorporates piëzo elements to vibrate a specially fabricated cantilever, with a tip that is only a few atoms thick, near its resonance frequency and a given oscillation amplitude. For surface profiling the AFM is most commonly in 'tapping mode', which means that both the frequency and the amplitude are kept constant. A laser is directed on the cantilever and the reflection of that laser is pointed at an array of photo-diodes that measure its vertical deflection. The cantilever is guided along the sample in a raster where the tip will be repelled by the Van der Waals and electrostatic forces of the atoms on the substrate when it gets too close. The resulting change in oscillation amplitude triggers a reaction from an electric servo motor to regain the original amplitude by moving up and/or down. The image of a surface profile (fig. 5.2) is therefore formed by mapping the force between the tip and the sample surface. The profilometer was at some point not operational due problems with a technical nature, measuring the thickness was then done with the AFM. The measured thickness and T_c of the sputtered films are displayed in fig. 5.5.

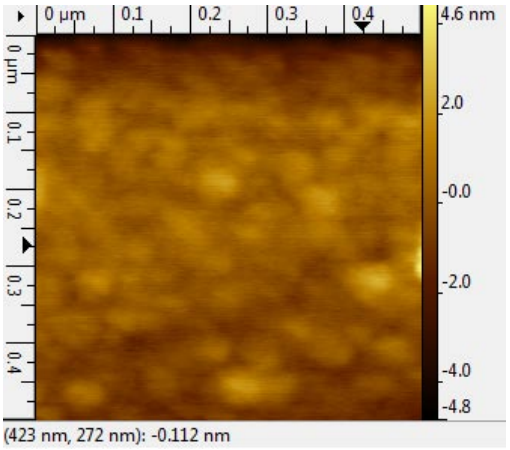

Figure 5.2: Surface profile of NbTiN made with an AFM.

5.2 Plasma power

To attract the positive argon ions (Ar^+) and create the bombardment a negative voltage is applied on the target. The power (P) is given by the voltage (U) times the current (I) squared: $P = U \cdot I^2$. The power supply generates 1A so the voltage will be the same number as the power in W. Therefor the negative voltage applied to the target is usually referred to as 'plasma power'. Lower plasma power will attract the Ar^+ with less force and thus the target atoms will continue to the substrate surface with less speed. This will result in a lower deposition rate and the idea is to test whether this also results in a higher film density, uniformity and T_c. The power on both targets will also determine how much Nb and Ti are sputtered on the substrate. An ideal ratio is seen in Iossad's [23] thesis ($\tilde{3}0$ percent Ti). Niobium has an atomic mass about twice of titanium. During sputtering titanium and nitride will bond and form titanium nitride (TiN) which is a ceramic. For this reason titanium is sputtered with the RF power source. From fig. 5.1 we can see that the thickness of thin films has substantial influence on the T_c of that film, especially at a thickness < 70 nm. Samples R04-R06 were sputtered with changing amount of power on the Ti target, resulting in a lower deposition rate and thus thickness. The T_c goes down with less Ti in the sputtered films but it can not be concluded if this is due to the thickness of the consistency of the film. Films were from this point sputtered to a thickness > 70 nm.

5.3 Substrate temperature

Under normal circumstances atoms that are randomly deposited by sputtering inherit a low mobility, they will stay put at the place they condensed, creating so-called ad-atoms. This low ad-atom mobility leads to atomic self-shadowing, trapping and retaining gas, causing a pillar like structure and micro voids. A solution to this is to increase the temperature of

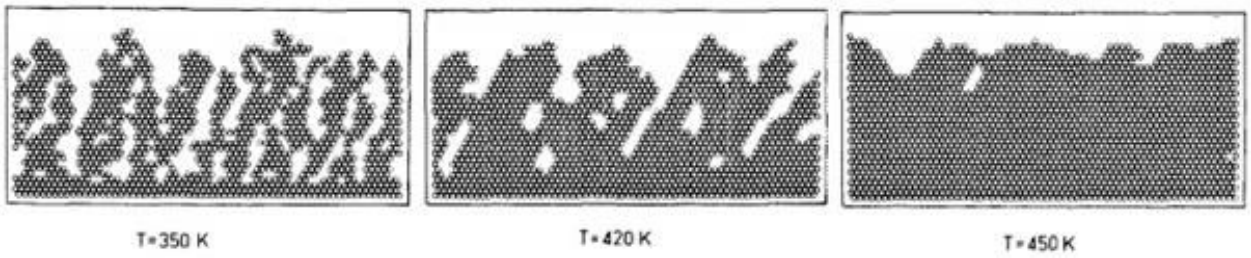

Figure 5.3: Higher temperature during deposition allows condensed atoms to move and create a film with a more uniform composition [35].

the substrate so condensed ad-atoms have enough mobility to wiggle into place as can be seen in fig. 5.3. The sputter machine is capable of reaching 850° C. For NbN films higher substrate temperature has a positive effect on the T_c [36]. To map the influence of substrate temperature on NbTiN, films will be created in steps of 50° C from room temperature (T_r) to 800° C. Clearly samples sputtered with a temperature of 600° C (R10, 14.3 K) have higher T_c than samples sputtered at room temperature (R08, 11.3 K). R08 has a higher thickness but this does not compensate for the lack in T_c.

Figure 5.4: Parameters used to sputter different samples. Power on both targets and the substrate temperature were altered to see the effect of these changes on the critical temperature of the created films.

Sample	$p_{sputter}$ (± 0.1 mTorr)	Argon flow (± 0.1 sccm)	Nitrogen flow (± 0.1 sccm)	P_{Ti} (± 0.1 W)	P_{Nb} (± 0.1 W)	$T_{substrate}$ (± 0.5 °C)	$t_{sputter}$ (± 0.5 s)
R01	3.0	50.0	5.0	250	200	21	180
R02	3.0	50.0	5.0	250	200	600	180
R03	3.0	50.0	5.0	200	200	21	180
R04	3.0	50.0	5.0	175	200	21	180
R05	3.0	50.0	5.0	150	200	21	180
R06	3.0	50.0	5.0	125	200	21	180
R07	3.0	50.0	5.0	225	200	21	180
R08	3.0	50.0	5.0	200	200	21	840
R09	3.0	50.0	5.0	200	175	21	1080
R10	3.0	50.0	5.0	200	200	600	700
R11	3.0	50.0	5.0	200	150	21	1135
R12	3.0	50.0	5.0	200	125	21	1437
R13	3.0	50.0	5.0	200	100	21	-

Figure 5.5: Measured thickness and T_c of the sputtered samples.

Sample name	Rate (± 0.05 Å s^{-1})	Thickness (± 0.1 nm)	T_c (±0.1K)
R01	0.7	9.8	-
R02	0.6	9.2	11.4
R03	1.1	18.9	-
R04	0.9	16.3	11.3
R05	0.8	14.8	10.8
R06	0.9	16.3	10.4
R07	1.1	18.7	-
R08	0.9	80.4	11.3
R09	0.7	80.2	10.7
R10	1.0	70.0	14.3
R11	0.6	70.0	10.8
R12	0.5	70.0	11.4
R13	-	70.0	10.7

Chapter 6

Conclusion and future work

6.1 Conclusion

Sputtering is a process which can be influenced in many ways. This is both its strength and its weakness. The strength is that the properties of the final product can be controlled very precisely, but with many parameters controllable come many parts to control them. Parts like the water cooling inside the main chamber can break and make the system not usable for the creation of thin films.

The system that was designed for the measurement of the T_c of the sputtered thin films is operational. The Samples and temperature sensor are placed on a circle centered with the axis of the cold head, which guarantees that the sensor reads out the same temperature as experienced by the samples. To do that, the temperature sensor is also placed directly at a sample spot. This is important to reliably compare the samples to each other.

As the T_c of superconducting films greatly depends on the thickness of that films in the sub 70 nm region, films should be made thicker than 70 nm. This way they almost do not depend on this parameter and can be related to one another with higher accuracy. Higher substrate temperature during sputtering results in films with higher critical temperature.

6.2 Future work

6.2.1 Measurement setup

At the moment the heating element is placed on top of the mounting, the wires going to and from this element are hanging down between the mounting and the 40K shield. When loading and unloading samples this wiring is inconvenient. A new design with bigger sample space would allow bigger samples to be loaded, and would result in lower dependence on the sample geometry.

6.2.2 Sputter parameters

Due to the leak in the water pipe near the Nb target not enough samples could be created to give a definitive answer to the optimal parameters needed to produce NbTiN films with the higherst T_c. The parameters in the created films are however diverse, a trend could clearly be seen in both thickness and substrate temperature. When the sputter machine is operational again more films could be sputtered to identify the exact optimum for each parameter.

The flow of argon- and nitrogen gas constitute the plasma can both be controlled independently. A certain ratio of these gases can thus be allowed inside the main chamber. This ratio is important because there needs to be enough argon in the main chamber to start the ion bombardment and just enough nitrogen to properly start reacting with the niobium and titanium on the substrate surface to form (NbTi)N [23]. The ideal ratio between these gasses should be examined as it could have a positive influence on the critical temperature.

When the film is growing it tends to trap impurities like argon ions or sometimes micro voids; small pockets where there is no material [24]. The quality of the film will decrease if the

amount of trapped impurities increases. A bulk film with minimal impurities can be created by applying a negative BIAS voltage on the substrate [25]. This negative voltage will, like on the target, attract the A^+ from the plasma to bombard the atoms into a uniform film. Both the increased substrate temperature and the voltage on the substrate have the effect of a more uniform film, however the atoms wiggle gently into place when the substrate temperature is increased, whereas they are pushed into place violently with the added voltage. Expected is thus that the surface roughness is more smooth with the higher temperature. Films should be made with different electric fields applied and their composition and surface profile should be checked and compared to films created with increased temperature to find an optimum.

Bibliography

[1] Plasma: *Introduction to Plasma Physics and Controlled Fusion 2nd Edition Volume 1*, Francis F. Chen, ISBN 0-306-41332-9 (1984).

[2] Klaus P. Almtoft: *Structural Characterization of Nanocrystalline Thin Films Grown by Magnetron Sputtering* PhD Thesis (2006).

[3] Turbo molecular pump: *https://en.wikipedia.org/wiki/Turbomolecular_pump*, visited may 9 2016.

[4] Roughing pump: *https://en.wikipedia.org/wiki/Roughing_pump*, visited may 9 2016.

[5] Cascade ionisation process: Edbertho Leal-Quirós, *Plasma Processing of Municipal Solid Waste*, Brazilian Journal of Physics, vol. 34, no. 4B (2004).

[6] Measuring deposition rate: *https://en.wikipedia.org/wiki/Quartz_crystal_microbalance*, visited 2 March 2016.

[7] Sauerbrey's equation: *https://en.wikipedia.org/wiki/Sauerbrey_equation*, visited 2 March 2016.

[8] M. Jones: *Accurate Temperature Sensing with an External P-N Junction*, Lineair Technology, application note 137 (May 2012).

[9] Substrate heater: *http://www.ajaint.com/substrate-heaters.html* visited 14 March 2016.

[10] Temperature control module: Model ETR-9300 Microprocessor Based SMARTER LOGIC Temperature Control Instruction Manual number 32.

[11] Niobium target information: *http://www.lesker.com/newweb/deposition_materials/depositionmaterials_sputtertarget* visited 14 March 2016.

[12] Stycast 2850FT Epoxy, technical data sheet: *http://research.physics.illinois.edu/bezryadin/labprotocol/stycast2850.p* visited May 16 2016

[13] Titanium target information: *http://www.lesker.com/newweb/deposition_materials/depositionmaterials_sputtertarge* visited 14 March 2016.

[14] Cryo-Torr Cryopump Manual: *Pub. No. 8040613, Rev. AA, 01/14/2013 ECO No. 63723*, 2013 Brooks Automation Inc.

[15] RF sputtering: P.J. Kelly et al. *Magnetron sputtering: a review of recent developments and applications*, Vacuum 56 (2000) 159-172.

[16] R.P. van der Molen: *Creating the optimal NbTiN thin films* Internship report from internship at Quantum Transport group at TU-Delft (2014).

[17] Sputtering system: *http://www.ajaint.com/sputtering-systems.html*, visited 16 Feb 2016.

[18] Sputter process: *http://www.ajaint.com/what-is-sputtering.html*, visited 16 Feb 2016.

[19] Cooper pairs (figure [19] *http://www.bookofjoe.com/2008/01/is-consciousnes.html*, visited april 1 2016.

[20] Pictures of sputtering process: *http://marriott.tistory.com/77*, visited 15 Feb 2016.

[21] Boltzmann's constant: *https://en.wikipedia.org/wiki/Boltzmann_constant*, visited 31 March 2016.

[22] J. Bardeen, L.N. Cooper and J.R. Schrieffer: *Theory of Superconductivity*, Physical Review, volume 108, number 5 (1957).

[23] N. Iossad, *Metal Nitrides for Superconducting Tunnel Detectors*, PhD Thesis (2002).

[24] Maissel et al,: *Thin Films Deposited by Bias Sputtering*, Journal of Applied Physics 36, (1965).

[25] Robert K. Waits: *Thin film deposition and patterning*, American Vacuum Society (1998).

[26] P.C. Lanchester: *Digital thermometer circuit for silicon diode sensors*, Cryogenics, Vol 29, pages 1156-1159 (1989).

[27] Quad twisted cryogenic wire's: *http://www.lakeshore.com/products/Cryogenic-Accessories/Wire/pages/Specifications.aspx "QT 36"*, visited 6 april 2016.

[28] Fisher connectors: *http://www.fischerconnectors.com/sites/default/files/specifications/fischer_core_series_brass_techs* visited 6 april 2016.

[29] Lessons In Electric Circuits, Volume I DC, chapter 8.9 "Kelvin (4-wire) resistance measurement" page 282-288 by Tony R. Kuphaldt, fifth Edition (2006). Accesed from:

http://www.allaboutcircuits.com/textbook/direct-current/chpt-8/kelvin-resistance-measurement/ on 4 april 2016.

[30] F.M. Smits: *Measurement of Sheet Resistivities with the Four-Point Probe*, the Bell System Technical Journal, May 1958.

[31] Spring loaded pogo pins: *http://uk.rs-online.com/web/p/pcb-pin-socket-strips/7020109/*, visited april 6 2016.

[32] Oxigen free high conductivity copper: *https://www.alfa.com/en/ofhc-oxygen-free-high-conductivity/*, visited april 6 2016.

[33] Keithley 2700 Multimeter/Switch System: *Users manual, Document Number: 2700-900-01 Revision F.*

[34] Keithley 7700 20-channel, Differential Multiplexer Module: *Keithley 2700 User's Manual page 379.*

[35] K. Muller: *Dependence of thin film micro-structures on deposition rate by means of a computer*, Journal of Applied Physics, number 58 (1985).

[36] S.H. Bedorf: *Development of Ultrathin Niobium Nitride and Niobium Titanium Nitride Films for THz Hot-Electron Bolometers*, PhD Thesis (2005).

[37] Lei Yu et al.: *Fabrication of Niobium Titanium Nitride Thin Films With High Superconducting Transition Temperatures and Short Penetration Lengths*, Transaction on applied superconductivity, vol. 15, no. 1, march 2005.

[38] Bruker 'DektakXT' profilometer: *https://www.bruker.com/products/surface-analysis/stylus-profilometers/dektak-xt/overview.html*, visited 26 april 2016.

[39] Bruker 'Dimension FastScan' Atomic Force Microscope: *https://www.bruker.com/products/surface-analysis/atomic-force-microscopes/dimension-fastscan/overview.html*, visited 26 april 2016.

[40] Carbon ceramic resistor thermometer: CCS/A2 from Temati Cryogenics, *http://www.temati-uk.com/html/ccs_sensors.html*, visited May 2 2016.

[41] G. Binnig et al.: *Atomic Force Microscope*, Physical Review Letters, volume 56 number 9 (1986).

[42] Sumitomo Heavy Industries *http://www.shicryogenics.com/products/4k-cryocoolers/rdk-101d-4k-cryocooler-series/*, visited 17 Feb 2016.

[43] Lakeshore temperature controller: *http://www.lakeshore.com/products/Cryogenic-Temperature-Controllers/Model-331/Pages/Overview.aspx*, visited april 1 2016.

[44] Quad-Twist cryogenic wire: *http://www.ti.com/lit/an/sboa019/sboa019.pdf*, visited 18 April 2016.